MATERIALE PLASTICE
https://revmaterialeplastice.ro
https://doi.org/10.37358/Mat.Plast.1964

Percolation Effects in MCNT-filled Polystyrene: Rheological, Optical, Adhesion and Conductive Investigations

ANDREEA IRINA BARZIC*
"Petru Poni" Institute of Macromolecular Chemistry, 41A Grigore Ghica Voda Alley, 700487, Iasi, Romania

Abstract: *This work is devoted to the preparation and characterization of some polystyrene/multiwall carbon nanotubes (PS/MCNT) systems. The dispersion of the reinforcement agent within the PS medium was done via sonication and the resulting nanocomposites containing 0-40 wt% MCNTs were achieved by solution blending procedure. Shear flow and viscoelastic properties were tested by means of rheology, revealing some changes in the sample microstructure. Dispersion curves of the matrix and low filled nanocomposite were registered at variable temperatures. The theoretical refractive index and corresponding dielectric constant at optical frequencies were analyzed as a function of the system composition. Heat transport in the reinforced materials was examined by computer modeling, which enabled calculation of thermal conductivity. Electrical transport features were assessed using a theoretical approach relying on the physical properties of each phase. The surface adhesion of the samples with various materials was determined to check the suitability for applications in technical or bio-related fields.*

Keywords*: polystyrene, carbon nanotubes, percolation, shear flow, adhesion, conduction*

1. Introduction

Multiwall carbon nanotubes (MCNT) are widely employed as reinforcement agents for plastics to enhance their performance in terms of lightweight, mechanical resistance, hydrophobicity, electrical and thermal conduction abilities [1,2]. This advantageous combination of properties is highly desirable for a large range of applications, such as flexible electrodes, radiation shielding sheets, heat dissipation layers, selective sensors, membranes and energy conversion devices [3,4]. Development of such multiphase materials depends upon characteristics of the inserted fillers, their dispersion state within the polymer environment, the interactions occurring between reinforcement compound and the plastic material used as matrix [5,6]. There are many fabrication processes of the carbon nanotubes/polymer nanocomposites, such as: solution blending, melt compounding, sol-gel, in situ and polymerization method [7]. In the preparation stage, the effective appearance of the macroscopic conducting network inside the polymer bulk is shown to be essential for the improvement of the desired physical properties of nanocomposites. As a result, a careful attention must be given to the processing routes involved in obtaining the final material.

Generally, there are two major aspects that are discussed in the majority previous reports: dispersion of the reinforcement agents in the polymer matrix and their interactions that ensure the compatibility of the system. Concerning the first problem, the forces acting at the molecular scale among the fillers must be accounted owing to the high surface-to-mass ratio of carbon nanotubes. Van der Waals forces frequently favor flocculation of the reinforcement agents, whereas the steric effects and even electrostatic charges produce stabilization of the dispersion via repulsive forces [8]. Therefore by elucidating the nature of percolating network made by MCNT, the balance of the two aspects of the aforementioned opposite effects must be considered. Regarding the other issue, it was evidenced that the fillers in the polymer medium are covered or encapsulated with a thin insulating matrix layer [9,10]. Such encapsulation can be viewed as a barrier to the electrical charge transport among the fillers [9]. Each nanocomposite displays a percolation threshold, which is affected by the processing conditions, matrix type, filler size, filler functionalization and so on. In the case of the carbon nanotubes, the

email: irina_cosutchi@yahoo.com

disruption of bundles and their distribution in the matrix determine the performance of the nanocomposite especially in terms of conduction properties.

Among the polymers used in nanocomposite synthesis, polystyrene (PS) is one of the most utilized plastics owing to its ease of processing, high hydrophobicity, good mechanical resistance, transparency and low costs. PS/MCNT nanocomposites have been described in some research studies [11-25], which emphasize new methods of synthesis, effects of CNT functionalization, methods of processing and impact of nanofillers orientation and percolation on the physical properties.

The motivation for the present paper is given by the possible use of PS/MCNT as heat dissipation layers in high power electronics, electromagnetic interference shielding (EMI) materials or components for blood-contacting or cell monitoring devices. Rheological tests were conducted to analyze the microstructural changes upon MCNT filling and the sample's response to deformation. Morphological features of the PS containing low amounts of MCNT were made using optical microscopy. Adhesion studies of the obtained nanocomposites to various materials encountered in these applicative fields were performed. Optical, thermal and electrical properties were also investigated in regard to pursued purposes.

2. Materials and methods

2.1. Materials and sample preparation

Polystyrene (PS) of 10 000 Da molecular mass, multiwall carbon nanotubes (MCNT, diameters of ~6 nm and ~20 nm, length of ~20 μm) and the solvents dimethylacetamide (DMAc, anhydrous, 99%), methylene chloride (MC) were purchased from Sigma Aldrich.

The samples were prepared by solution blending method. First, a dispersion of a precise content of MCNT (1-40 wt%) in DMAc was subjected to sonication for several hours. Secondly, a PS solution in 50/50 DMAc/MC was prepared under magnetic stirring for proper homogenization. Then, the two solutions were mixed and the homogenous mixture was casted on clean substrates, while left to dry at temperatures above 160°C in a vacuum oven.

2.2. Characterization

Rheological experiments of polymer solution having a concentration of 10% are registered on a cone-plate rheometer at room temperature. Shear viscosity was registered in the 0.01-300 s^{-1} range, while oscillatory tests were made in 0.1-16 Hz.

Refractive index of PS and PS/MCNT films at low filler contents was determined on an Abbe refractometer at several temperatures.

Simulation of the heat transfer in the composite was achieved with Ansys software (demo version).

Electrical conduction of samples was determined on a Keithley device.

The morphology of unfilled and low reinforced polymer films was recorded using an optical microscope from Bresser.

3. Results and discussions

3.1. Rheological behavior

The solution properties under shearing were evaluated by rheological tests as depicted in Figure 1. Shear flow curve of the unfilled PS solution in DMAc/MC presents a Newtonian plateau at shear rates between 0.01-10 s^{-1}, afterwards a shear thinning zone is observed due to chain disentanglements and orientation. Newtonian flow of the PS (of higher molecular mass) was also reported for solutions in DMAc or dimethylformamide and for the latter solvent the shear thinning follows after the constant viscosity domain [16, 26]. Upon MCNT reinforcement, the low shear rate behavior is gradually changed from Newtonian to shear thinning. Thus, the overall value of the viscosity increases, but becomes more sensitive to the applied shear rate as the amount of filler increases. This aspect reveals that the presence of the carbon reinforcement agent in the PS solution determines important changes in the sample microstructure. In order to elucidate them, shear viscometry experiments are further continued, with

shear oscillatory measurements in the linear viscoelastic regime. The dependence of rheological moduli on shear frequency (*f*) is illustrated in Figure 2(a) for PS solution and the corresponding MCNT-filled solutions. The pristine PS sample behaves like a viscoelastic fluid, displaying a power law frequency dependence of both storage (G') and loss (G") modulus, without any plateau appearing during flow. At low frequencies, one may remark that G" ~ f^2 and G' ~ f^1, while as the frequency is enhanced the storage modulus progressively increases until a point that exceeds the viscous modulus. This marks the overlapping frequency, which is related to the relaxation time. As noticed in Figure 2(a), the overlapping point for the pristine PS sample is 3.09 Hz. By comparison the rheological moduli variation with applied frequency is presented for the highest level of reinforcement, namely PS/MCNT 40 wt%, and differences in the rheological response are noted. At low frequencies one may observe a plateau showing that the percolated MCNT is forming a pseudo-solid-like network characterized by powerful interactions between filler and host [16]. Evidence of its appearance relies on the following aspect: the pure PS sample presents a transition from elastic to viscous behavior and after 3.09 Hz the specimen presents predominantly elastic response along the high frequencies range, while for the reinforced PS, the prevalent elastic properties at low frequencies up to 10.78 Hz, are remarked. The transition point of the nanocomposite solutions is noted at a higher frequency, which is indicative of a smaller relaxation time in regard to the pristine PS sample. The latter is because in the composite solution microstructure is modified by the appearance of a more elastic percolated network and this is why the elastic modulus is suddenly changed by the filler amount inserted in the system (Figure 2(b)).

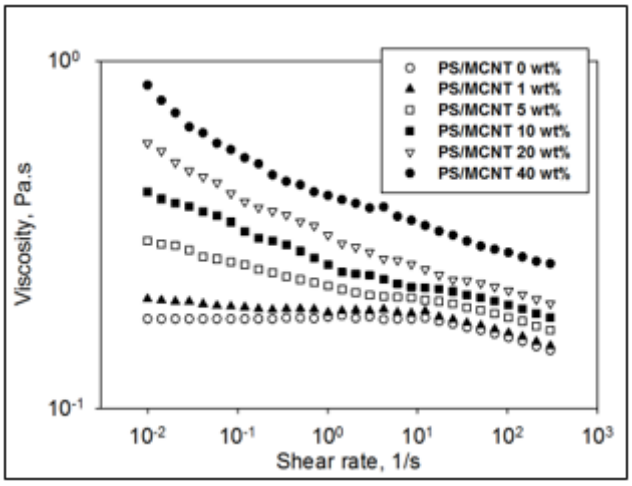

Figure 1. Shear flow curves for MCNT-filled PS solutions at room temperature

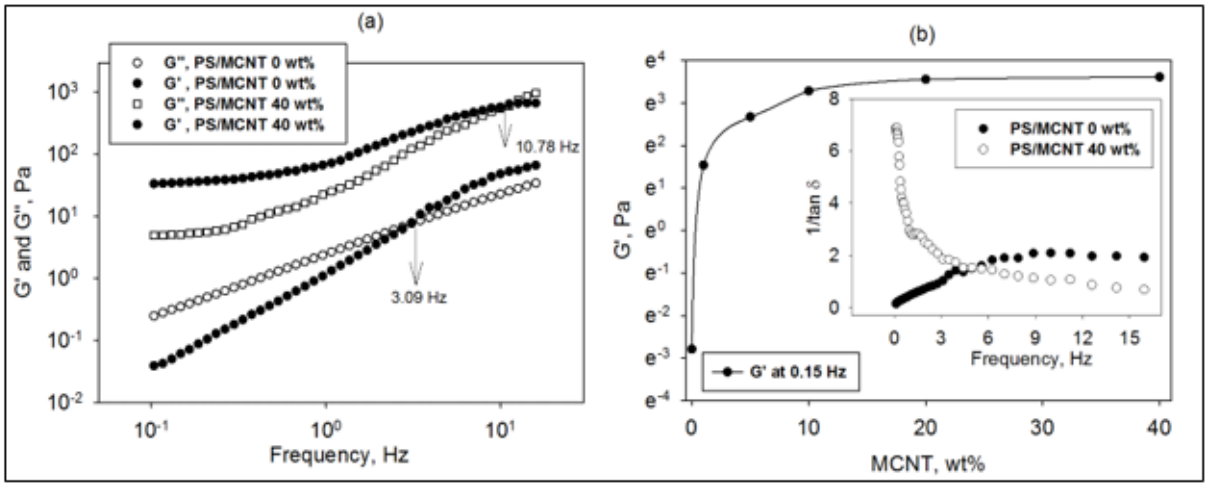

Figure 2. Shear moduli against frequency (a) and storage modulus against filler amount (b) for PS/MCNT nanocomposites

Supplementary insight into filler-host interactions can be achieved from inverse loss tangent (1/tan δ), which is known to show information on the sample damping characteristics [16]. As indicated in the inset image from Figure 2(b), the values of the 1/tan δ increase in the presence of the MCNT in the PS matrix, particularly at low frequencies, revealing a hindrance to energy dissipation and relaxation of the macromolecular chains owing to the percolation of the filler. Similar results were reported by Kota et al [16], which also report that firmness of the PS changes upon the reinforcement with the MCNT. From the point of view of the sample microstructure, they prove that the elastic load transfer and electrical properties could be considered of higher sensitivity to the onset of the percolated filler in comparison with the viscous dissipation mechanisms as shown by the modification in the power-law exponent [16]. Solution processing of the matrix is more adequate for spin coating, while doping of the PS sample determines a rheological behavior more suited for processing into films via the tape casting technique.

3.2. Morphological and adhesion analysis

Optical microscopy was used to examine the morphological features of the PS matrix and its composites with MCNT. According to the Figure 3(a), the studied polymer film displays a porous surface. Given the fact that at 1 wt% filler in the PS the sample is still transparent, it was possible to investigate by microscopy (in transmission mode) the level of MCNT dispersion in the system. As remarked in Figure 3(b), the reinforcement agent is well distributed inside the polymer medium. Further PS filling reduces the sample clarity and thus is no longer possible to characterize these materials by methods that impose optical clarity, like optical microscopy.

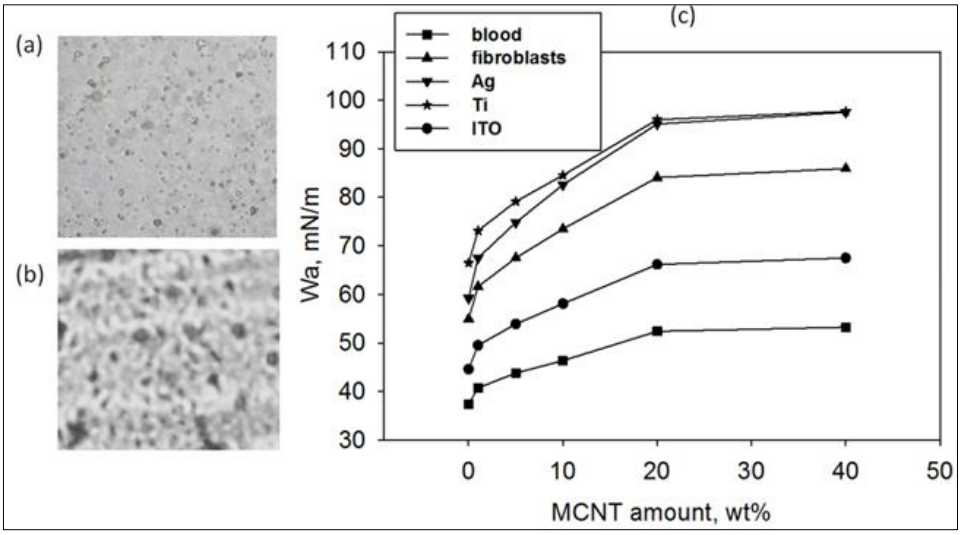

Figure 3. Optical mcroscopy images of (a) PS matrix, (b) PS/MCNT 1wt% and (c) sample adhesion work against filler amount with various materials

The morphological aspects are not the only ones that influence the adhesion properties, so the surface tension characteristics must be also investigated. Literature [27] shows that polystyrene presents a higher disperse component of the surface tension in regard to the polar one. This aspect is reflected in the adhesion properties of the PS and PS/MCNT with other materials of interest in high power electronics, EMI or biomedical devices. The adhesion data from Figure 3(c) are calculated on the basis of surface tension of the obtained composite samples and those of some selected materials (blood, fibroblasts, Ag, Ti, ITO) [28-31], using equation (1):

$$Wa = 2 \cdot \left(\sqrt{\gamma_s^d \gamma_m^d} + \sqrt{\gamma_s^p \gamma_m^p} \right) \quad (1)$$

where Wa is the adhesion work, γ is the surface tension, the subscripts "s" and "m" represent the sample and the interacting material and the superscripts "d" and "p" denote the dispersive and polar surface tension.

The dispersive surface tension of the prepared samples ranges with increasing filler content as follows: 19.54 mN/m (0 wt%), 26.02 mN/m (1 wt%), 32.47 mN/m (5 wt%), 40.40 mN/m (10 wt%), 54.01 mN/m (20 wt%) and 57 mN/m (40 wt%). On the other hand, the polar component of the film samples is varying as follows: 0.42 mN/m (0 wt%), 0.30 mN/m (1 wt%), 0.22 mN/m (5 wt%), 0.1 mN/m (10 wt%), 0.071 mN/m (20 wt%) and 0.05 mN/m (40 wt%). Figure 3(c) shows the variation of the adhesion work of the studied samples with filler content. Some biomedical devices involve the utilization of hemocompatible and/or cytocompatible materials. The smallest work of adhesion is noted for blood, however for blood contacting materials this is not a good result since blood must not adhere to the contact layer. Conversely for the case of fibroblasts, the good adhesion to the prepared nanocomposites recommends them as components for device made for cell growth monitoring (e.g. neuronal recovery). In high power electronics the nanocomposite would be interfaced with metallic components, so the high adhesion with Ti, Ag or ITO (indium tin oxide) observed in Figure 3(c) is adequate for pursued applications. Regardless the considered material, work of adhesion increases with MCNT amount in PS for all analyzed composites.

3.3. Refractive index and dielectric constant

The refractive index (n) of the transparent samples (PS and PS/MCNT 1 wt%) was determined by means of refractometry at several temperatures (Figure 4). The PS/MCNT film samples display normal dispersion curves. While the temperature increases, one may observe the reduction of the refractive index, the introduced filler in the PS generating the enhancement of the refractive index values. For the other reinforced samples, this optical parameter was determined by group contribution approach, knowing the values for both PS and MCNT [32]. The theoretical values of the refractive index (n_{theor}) are grouped in Table 1 and show a good concordance for the experimental values of the PS and PS/MCNT 1 wt% samples from Figure 4.

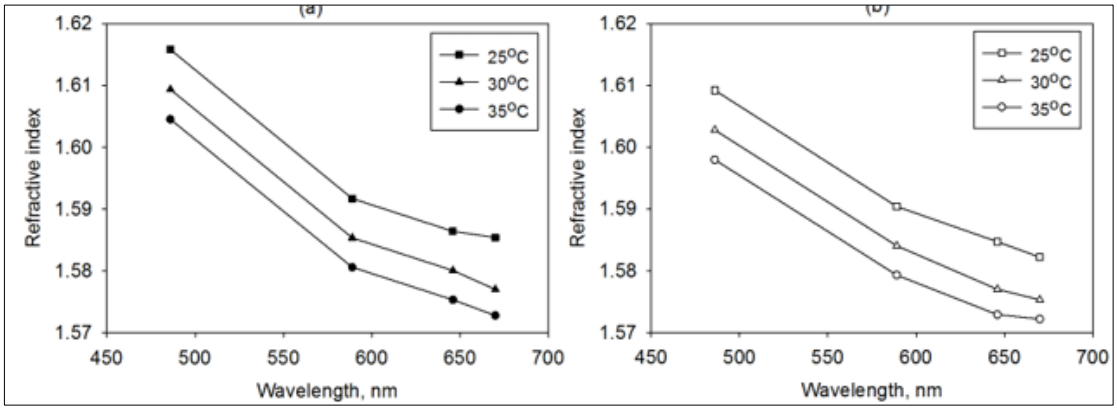

Figure 4. Refractive index dispersion at several temperatures of (a) pure PS and (b) PS/MCNT 1 wt%

The refractive index is an important parameter that provides information on the band gap energy (Eg), dielectric constant (ε) at optical frequencies and first order optical susceptibility (χ [1]). The values of ε and χ [1] can be determined from the Maxwell equation (2) and from the data extracted from Wemple and DiDomenico (WDD) model [33] - equations (3-4), respectively:

$$n_{theor} = 1.1\ \varepsilon^2 \quad (2)$$

$$n^2 = \frac{E_0^2 - (h\nu)^2 + E_d E_0}{E_0^2 - (h\nu)^2} \quad (3)$$

$$\chi[1] = (E_d / E_0) \cdot (1/4\pi) \quad (4)$$

where h is the Planck's constant, ν is the frequency, E_0 denotes the single-oscillator energy for electronic transitions and E_d is the dispersion energy.

The results are listed in Table 1, revealing that the addition of the MCNT particles decreases the magnitude of the band gap energy of the nanocomposite. Such aspect could be useful for enhancing the conduction properties of the samples. Moreover, the improvement of the dielectric constant is good for energy storage applications, knowing that the storage energy is proportional to the sample permittivity.

Table 1. The values of the refractive index, dielectric constant, band gap energy, dispersion energy, single-oscillator energy and optical susceptibility for the pristine PS and its MCNT nanocomposites

Sample	Parameter					
	n_{theor}	ε_{theor}	E_g (eV)	E_d (eV)	E_0 (eV)	χ[1]
PS/MCNT 0 wt%	1.592	2.787	4.020	9.114	8.040	0.090
PS/MCNT 1 wt%	1.594	2.794	4.016	9.253	8.032	0.092
PS/MCNT 5 wt%	1.602	2.823	4.003	-	-	-
PS/MCNT 10 wt%	1.613	2.860	3.986	-	-	-
PS/MCNT 20 wt%	1.633	2.935	3.953	-	-	-
PS/MCNT 40 wt%	1.675	3.086	3.885	-	-	-

3.4. Thermal and electrical conductivity

The heat transport in the PS/MCNT nanocomposites was assessed by simulation with Ansys software based on the finite element method. In a previous work [14] such data were reported for the case of one MCNT in PS, emphasizing the effects of nanofiller orientation in the polymer. Here, it is shown the effect of filling level of the PS on the thermal transport properties. The settings made for achieving the steady state response also involve the establishment of the thermal boundaries, and afford the user to choose elements designed to process thermal calculations. The boundary settings are enforced to limit the heat flow to the one axis. By applying the adequate tools in the analysis package, the heat flux and thermal gradient at all nodes of the meshed volume is computed (Figure 5).

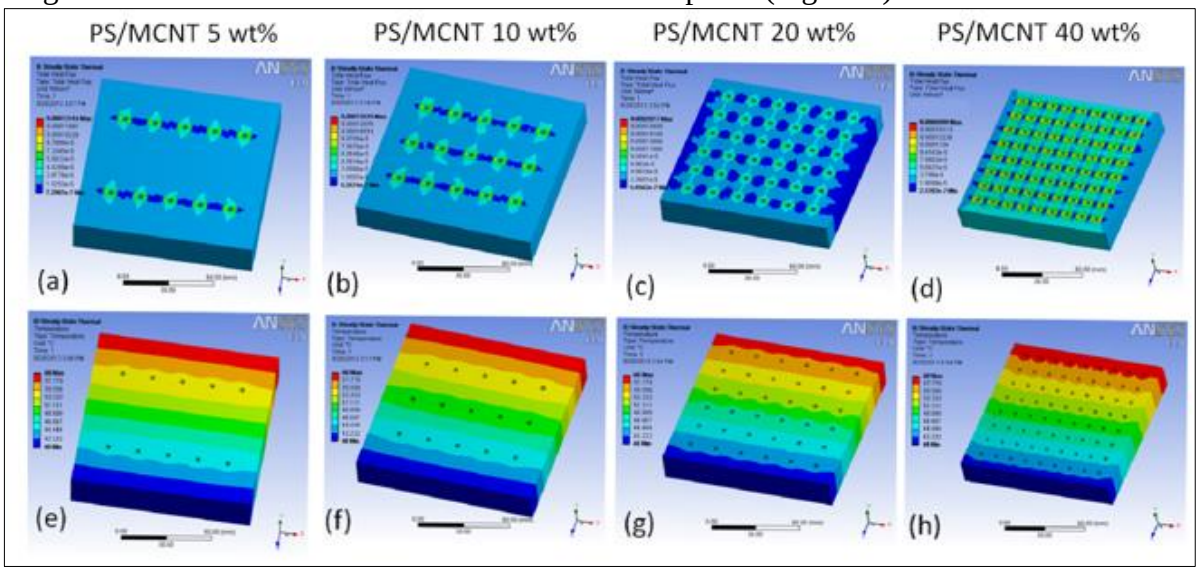

Figure 5. The heat flux (a)-(d) and thermal gradient (e)-(h) for PS filled with various levels of MCNT

The average heat flux and the thermal gradient are determined. As proposed by Fourier law for thermal conduction, the aforementioned parameters are mandatory for estimation of the thermal conduction as seen in the equation (5). The results for q, dT/dx and k are listed in Table 2.

$$q = - k \cdot (dT/dx) \quad (5)$$

where q denotes the heat flux, k is the thermal conductivity and the term dT/dx represents the thermal gradient.

Table 2. The values of the heat flux, temperature gradient, thermal and electrical coductivity for the pristine PS and its MCNT nanocomposites

Sample	Parameter			
	q (W/m^2)	dT/dx (K/m)	k (W/m K)	σ (S/m)
PS/MCNT 0 wt%	-	-	0.135*	$2.21 *10^{-18}$
PS/MCNT 1 wt%	-	-	1.435*	$1.58 *10^{-4}$
PS/MCNT 5 wt%	58.82	49.99	1.177	$4.37*10^{-2}$
PS/MCNT 10 wt%	68.16	49.99	1.363	$3.55*10^{-1}$
PS/MCNT 20 wt%	104.15	49.99	2.083	1.829
PS/MCNT 40 wt%	349.62	49.99	12.995	3.767

* values from ref. [14]

It can be remarked that the thermal conductivity of the unfilled PS is very low, namely 0.135 W/ m K as previously reported [14]. Upon MCNT doping, the thermal conduction in the nanocomposites is gradually enhanced. Analysis of the data from Table 2 confirms the formation of a percolation network in the samples, as seen in rheological data. Litoiu et al [34] also studied the heat transfer in such nanocomposites and confirmed the improvement of the thermal conductivity of the polymers via MCNT addition. The augmentation of the heat transfer in the prepared multiphase materials is suitable for heat dissipation in high power electronic circuits.

Electrical conductivity (σ) is another important factor in electronic applications. Table 2 shows the electrical performance of the studied materials. The values are in agreement with literature [16,35,36], which reveal an exponential increase of σ upon insertion of the MCNT. Knowing from literature [37] that the EMI shielding effectiveness is a function of electrical conductivity, it can be stated that the prepared nanocomposites can be used for such applications.

4. Conclusions

PS and PS/MCNT composites were prepared by solution casting. The rheological properties reflect the formation of a percolation network in the polymer matrix. Such microstructural changes are impacting optical, dielectric, adhesion and conduction properties. The enhancement of the dielectric properties is suitable for high energy density materials or electromagnetic shielding. Sample adhesion with blood is not good for blood contacting devices, while increase in the thermal transfer recommends the studied samples as heat dissipation elements in high power electronics.

Acknowledgments: Financial support of "Petru Poni" Institute of Macromolecular Chemistry from Romanian Academy is acknowledged.

References

1. MITTAL, G., DHAND, V., RHEE, K.Y., PARK, S.J., LEE, W.R., A review on carbon nanotubes and graphene as fillers in reinforced polymer nanocomposites, *J. Ind. Eng. Chem.*, **21**, 2015, 11-25.
2. BHATTACHARYA, M., Polymer Nanocomposites - A Comparison between Carbon Nanotubes, Graphene, and Clay as Nanofillers, *Materials (Basel)*, **9**(4), 2016, 262.
3. HAN, Z., FINA, A., Thermal conductivity of carbon nanotubes and their polymer nanocomposites: A review, *Prog. Polym. Sci*., **36**, 2011, 914-944.
4. KAUSAR, A., RAFIQUE, I., MUHAMMAD, B., Review of Applications of polymer/carbon nanotubes and epoxy/CNT composites, *Polymer-Plast. Technol. Eng*., **55**(11), 2016, 1167-1191.
5. WANG, M.J., Effect of polymer-filler and filler-filler interactions on dynamic properties of filled vulcanizates, *Rubber Chem. Technol*., **71**(3), 1998, 520-589.
6. STANCIU, N.V., STAN, F., FETECAU, C., Melt shear rheology and pVT behavior of polypropylene /multi-walled carbon nanotube composites, *Mater. Plast*., **55**(4), 2018, 482-487.

7. TANAHASHI, M., Development of fabrication methods of filler/polymer nanocomposites: with focus on simple melt-compounding-based approach without surface modification of nanofillers, *Materials (Basel)*, **3**(3), 2010, 1593-1619.
8. OUNAIES, Z., PARK, C., WISE, K.E., SIOCHI, E.J., HARRISON, J.S., Electrical properties of single wall carbon nanotube reinforced polyimide composites, *Compos. Sci. Technol*., **63**(11), 2003, 1637-1646.
9. HU, G., ZHAO, C., ZHANG, S., YANG, M., WANG, Z., Low percolation thresholds of electrical conductivity and rheology in poly(ethylene terephthalate) through the networks of multi-walled carbon nanotubes, *Polymer*, **47**(1), 2006, 480-488.
10. MARTIN, A., SANDLER, J.K.W., SHAFFER, M.S.P., SCHWARZ, M.-K., BAUHOFER, W., SCHULTE, K., WINDLE, A.H., Formation of percolating networks in multi-wall carbon-nanotube–epoxy composites, *Compos. Sci. Technol*., **64**(15), 2004, 2309-2316.
11. PATOLE, A.S., PATOLE, S.P., YOO, J.-B., AN, J.H., KIM, T.H., Fabrication of polystyrene/ multiwalled carbon nanotube composite films synthesized by in situ microemulsion polymerization, *Polym. Eng. Sci*., **53**, 2013, 1327-1336.
12. BARZIC, R.F., STOICA, I., BARZIC, A.I., DUMITRASCU, G., Thermal properties of polystyrene/ carbon nanotubes composites prepared by shear casting, *Buletinul Institutului Politehnic Iasi Sectia Constructii de Masini*, **Tom LVIII (LXII)**, Fasc. 4, 2012, 59-64.
13. BARZIC, R.F., STOICA, I., GRADINARU, L.M. BARZIC, A.I., DUMITRASCU, G., Surface properties of some polystyrene-based nanocomposites, *Buletinul Institutului Politehnic Iasi, Sectia Matematica, Mecanica teoretica, Fizica*, **Tom LIX(LXIII)**, Fasc. 3, 2013, 35-40.
14. BARZIC, A.I., BARZIC, R.F., Thermal conduction in polystyrene/carbon nanotubes: effects of nanofiller orientation and percolation process, *Rev. Roum. Chim*., **60**(7-8), 2015, 803-807.
15. FRAGNEAUD, B., MASENELLI-VARLOT, K., GONZALEZ-MONTIEL, A., TERRONES, M., CAVAILLÉ, J.Y., Mechanical behavior of polystyrene grafted carbon nanotubes/polystyrene nanocomposites, *Compos. Sci. Technol*., **68**, 2008, 3265-3271.
16. KOTA, A. K., CIPRIANO, B.H., DUESTERBERG, M. K., GERSHON, A.L., POWELL, D., RAGHAVAN, S.R., BRUCK, H.A., Electrical and rheological percolation in polystyrene/MWCNT nanocomposites, *Macromolecules*, **40**, 2007, 7400-7406.
17. ZHOU, S., HRYMAK, A.N., KAMAL, M.R., Effect of hybrid carbon fillers on the electrical and morphological properties of polystyrene nanocomposites in microinjection molding, *Nanomaterials*, **8**, 2018, 779.
18. HILL, D. E., LIN, Y., RAO, A.M., ALLARD, L.F., SUN, Y.P., Functionalization of carbon nanotubes with polystyrene, *Macromolecules*, **35**, 2002, 9466-9471.
19. LIAO, K., SEAM, L.I., Interfacial characteristic of a carbon nanotubes-polystyrene composite system, *Applied Physics Letters*, **79**, 2001, 4225-4227.
20. QIAN, D., DICKEY, E. C., ANDREWS, R., RANTELL T., Load transfer and deformation mechanisms in carbon nanotube- polystyrene composites, *Applied Physics Letters*, **76**, 2000, 2868-2870.
21. GONG, P., WANG, G., TRAN, W.P., BUAHOM, P., ZHAI, S., LI, G., PARK, C.B., Advanced bimodal polystyrene/multi-walled carbon nanotube nanocomposite foams for thermal insulation, *Carbon*, **120**, 2017, 1-10.
22. KASEEM, M., HAMAD, K., KO, Y.G., Fabrication and materials properties of polystyrene/carbon nanotube (PS/CNT) composites: A review, *European Polymer Journal*, **79**, 2016, 36-62.
23. ZEIMARAN, E., AKBARIVAKILABADI, A., MAJUMDER, M., *Polystyrene Carbon Nanotube Nanocomposites, Handbook of Polymer Nanocomposites. Processing, Performance and Application*, K. Kar, J. Pandey, S. Rana, Springer, Berlin, 2015.
24. FU, D., KUANG, T., YEN, Y.C., LI, D., BENATAR, A., PENG, X.F., LEE, L.J., Polystyrene/multi-wall carbon nanotube composite and its foam assisted by ultrasound vibration, *J. Cell. Plast*., **53**(3), 2017, 273-285.

25. ESPINOSA-GONZÁLEZ, C.G., RODRÍGUEZ-MACÍAS, F.J., CANO-MÁRQUEZ, A.G., KAUR, J., SHOFNER, M.L., VEGA-CANTÚ, Y.I., Polystyrene composites with very high carbon nanotubes loadings by in situ grafting polymerization, *J. Mater. Res*., **28**(8), 2013, 1087-1096.
26. BARZIC, R.F., BARZIC, A.I., DUMITRASCU, G., Percolation effects on dielectric properties of polystyrene/$BaTiO_3$ nanocomposites, *U.P.B. Sci. Bull., Series A*, **76**(3), 2014, 225-234.
27. BARZIC, A.I., STOICA, I., BARZIC, R.F., Microstructure implications on surface features and dielectric properties of nanoceramics embedded in polystyrene, *Rev. Roum. Chim*., **60**(7-8), 2015, 809-815.
28.AGATHOPOULOS, S., NIKOLOPOULOS, P., Wettability and interfacial interactions in bioceramic -body-liquid systems, *J. Biomed. Mater. Res*., **29**, 1995, 421-429.
29. SOROCEANU, M., BARZIC, A.I., STOICA, I., SACARESCU, L., IOANID, E.G., HARABAGIU, V., Plasma effect on polyhydrosilane/metal interfacial adhesion/cohesion interactions, *Int. Adhes. Adhes*., **74**, 2017, 131-136.
30.STOICA, I., BARZIC, A.I., Butnaru M., Doroftei, F., Hulubei, C., Surface topography effect on fibroblasts population on epiclon-based polyimide films, *J. Adhes. Sci. Technol*., **29**, 2015, 2190-2207.
31.ZHONG, Z., ZHONG, Y., LIU, C., YIN, S., ZHANG, W., SHI, D., Study on the surface wetting properties of treated indium-tin-oxide anodes for polymer electroluminescent devices, Phys. Stat. Sol. (a) 198, 2003, 197-203.
32.PARK, S.J., OK, J.G., PARK, H.J., LEE, K.T., LEE, J.H., KIM, J.D., CHO, E., BAAC, H.W., KANG, S., GUO, L.J., Modulation of the effective density and refractive index of carbon nanotube forests via nanoimprint lithography, *Carbon*, **129**, 2018, 8-14.
33. DIDOMENICO, M., WEMPLE, S. H., Oxygen-Octahedra Ferroelectrics. I. Theory of Electro-optical and Nonlinear optical Effects, *J. Appl. Phys*., **40**, 1969, 720-734.
34. LITOIU, R., EDEN, M., BACU, C., GALUSCA, D.G., AGOP, M., Study on the Heat Transfer in Carbon Nanotube Composites with Polymer Matrix, *Mater. Plast*., **47**(4), 2010, 478-480.
35.CHEN, J., LIU, B., GAO, X., XU, D., A review of the interfacial characteristics of polymer nanocomposites containing carbon nanotubes, *RSC Advances*, **8**(49), 2018, 28048-28085.
36. QI, X.-Y., YAN, D., JIANG, Z., CAO, Y.-K., YU, Z.-Z., YAVARI, F., KORATKAR, N., Enhanced Electrical Conductivity in Polystyrene Nanocomposites at Ultra-Low Graphene Content, ACS *Applied Materials & Interfaces*, **3**(8), 2011, 3130-3133.
37.SAINI, P., ARORA, M., GUPTA, G., GUPTA, B.K., SINGH, V.N., CHOUDHARY, V., High permittivity polyaniline–barium titanate nanocomposites with excellent electromagnetic interference shielding response, *Nanoscale*, **5**, 2013, 4330.

Manuscript received: 16.10.2020